The diatom flora in the vicinity of the Pretoria Salt Pan, Transvaal, Republic of South Africa. Part III (final).

F.R. Schoeman, R.E.M. Archibald and P.J. Ashton
National Institute for Water Research, Council for Scientific and Industrial Research, Pretoria

This is the third and final contribution on the diatom flora recorded in the vicinity of the Pretoria Salt Pan. In the taxonomic section notes and illustrations (light and electron microscopy) are given for 19 of the 35 listed species.
S. Afr. J. Bot. 1984, 3: 191–207

Hierdie artikel is die derde en laaste oor die diatoomflora wat in die omgewing van die Pretoria Soutpan voorkom. In die taksonomiese afdeling word aantekeninge en illustrasies (lig- en elektronmikroskopies) vir 19 van die 35 gelyste spesies gegee.
S.-Afr. Tydskr. Plantk. 1984, 3: 191–207

Keywords: Diatomaceae, electron microscopy, morphology

F.R. Schoeman*, R.E.M. Archibald and P.J. Ashton
National Institute for Water Research,
Council for Scientific and Industrial Research,
P.O. Box 395, Pretoria, 0001 Republic of South Africa
*To whom correspondence should be addressed

Accepted 12 March 1984

Introduction

The hypersaline Pretoria Salt Pan with its saline artesian spring is the only example of a maar lake in southern Africa. Its morphometry and physico-chemistry were recently discussed by Ashton & Schoeman (1983). A paper dealing with the diatom flora of this floristically unknown system was also published (Schoeman & Ashton 1982a). The water sources of the farmlands (the Soutpan agricultural experimental farm) surrounding the salt pan and its crater consist of a perennial stream and several boreholes whose hydrochemistry is quite different from that of the spring feeding the Pretoria Salt Pan. Since the diatom flora of the surface waters in this area was virtually unknown, the diatoms recorded from these different water sources have been studied by light and, in certain cases, electron microscopy. The first results dealing with some of the taxa recorded from this area were published in two papers (Schoeman & Ashton 1982b; 1983). This is the final taxonomic paper in the series and deals with the remaining species.

Study area and sampling points

The Soutpan agricultural experimental farm is located at 25°24′S and 28°05′E in the Transvaal Province, South Africa (Schoeman & Ashton 1982b) and surrounds the volcanic crater with its saline lake, the Pretoria Salt Pan. Algal samples were collected from a stream, various open water reservoirs and cattle drinking troughs associated with several boreholes on the farm (full details of these sites are given in Schoeman & Ashton 1982b). Details of their chemical composition are provided in Schoeman & Ashton (1982b; 1983).

Materials and Methods

Methods for the preparation and examination of the diatom samples (light and electron microscopy) were previously presented (Schoeman & Ashton 1982b). The terminology used is that suggested by the Working Party on Diatom Terminology (Anon. 1975; Ross *et al.* 1979).

Observations and Discussion

The diatom species recorded in the vicinity of the Pretoria Salt Pan, which have not been discussed previously, are listed below. Several of these presented taxonomic problems and required detailed discussion. These species are therefore discussed in alphabetical order with notes on their

Table 1 Complete list of diatom species recorded in the vicinity of the Pretoria Salt Pan

Species Name	Sample Numbers								
	B1	B2	B3	B4	B5	B6	B7	B8	B9
Achnanthes engelbrechtii Cholnoky									X
A. exigua Grunow		X		X					
A. lanceolata Brébisson *ex* Kützing		X							
A. minutissima Kützing	X	X	X	X		X	X		X
Amphipleura pellucida (Kützing) Kützing	X	X							
Amphora ovalis (Kützing) Kützing var. *affinis* (Kützing) van Heurck *ex* De Toni		X							
A. veneta Kützing	X				X				
Brachysira exilis (Kützing) Round & Mann 1981 (as *Anomoeoneis exilis* in Schoeman & Ashton 1982b)									X
Cocconeis placentula Ehrenberg	X	X							
Cyclostephanos sp.									X
Cyclotella atomus Hustedt									X
C. meneghiniana Kützing					X				
Cymbella aspera (Ehrenberg) Peragallo		X							
C. cymbiformis Agardh	X	X							
C. kolbei Hustedt								X	
C. microcephala Grunow (Groups 1 and 2)	X		X						X
C. minuta Hilse *ex* Rabenhorst var. *silesiaca* (Bleisch *ex* Rabenhorst) Reimer		X							
Diploneis sp. [affin. *smithii* (Brébisson *ex* W. Smith) Cleve var. *pumila* (Grunow) Hustedt]		X							
Fragilaria construens (Ehrenberg) Grunow var. *venter* (Ehrenberg) Grunow									X
Gomphonema gracile Ehrenberg – *G. parvulum* (Kützing) Kützing complex		X			X				
Gyrosigma rautenbachiae Cholnoky		X							
Melosira granulata (Ehrenberg) Ralfs var. *angustissima* O. Müller		X							
Navicula cloacina Lange-Bertalot & Bonik		X							
N. cryptocephala Kützing		X							
N. cryptocephala Kützing complex		X			X				
N. maillardii Germain	X								
N. menisculus Schumann		X							
N. minima Grunow		X		X					
N. pupula Kützing		X							X
N. pygmaea Kützing		X							
N. sp [affin. *radiosa* Kützing]		X							
N. rostellata Kützing		X							
N. schroeteri Meister		X							
N. tenelloides Hustedt		X							
N. towutiensis Cholnoky					X				
N. zanonii Hustedt	X								
Nitzschia amphibia Grunow		X			X	X			
N. angusteforaminata Lange-Bertalot								X	
N. communis Rabenhorst	X								
N. denticula Grunow	X								X
N. dissipata (Kützing) Grunow		X							
N. fontifuga Cholnoky		X							
N. frustulum (Kützing) Grunow	X	X							
N. gracilis Hantzsch *ex* Rabenhorst						X	X		X
N. palea (Kützing) W. Smith complex		X		X			X	X	X
N. perminuta Grunow		X							
N. supralitorea Lange-Bertalot		X							
Rhopalodia gibba (Ehrenberg) O. Müller		X		X		X	X	X	X
R. gibberula (Ehrenberg) O. Müller		X							
Stauroneis anceps Ehrenberg				X					
Surirella ovalis Brébisson	X								
Synedra rumpens Kützing				X					
S. ulna (Nitzsch) Ehrenberg complex		X		X			X		
Thalassiosira weissflogii (Grunow) Fryxell & Hasle		X							

dimensions, taxonomy and valve morphology based on light and/or electron microscopical observation. In summary, a list of all species recorded in the vicinity of the Pretoria Salt Pan is presented in Table 1.

Cyclostephanos sp. (Figures 1–13)

Dimensions: specimens from sample B9 (Figures 1–5). Diameter 11,0–13,0 μm. Striae fascicles 9–10 in 10 μm. Marginal strutted processes 3–4 in 10μm.

Dimensions: specimens from Rietvlei Dam (Figures 6–13). Diameter 5,0–7,0 μm. Striae fascicles 15–18 in 10 μm. Marginal strutted processes 3–4 in 10 μm.

This taxon is rare in the vicinity of the Pretoria Salt Pan and only a few valves (Figures 1–5) were observed with LM in sample B9. This is unfortunate since the correct identity of many of these small centric diatoms can only be determined from the finer details of their valve morphology as seen with EM. Although we have no EM micrographs of this form, comparison of its morphological features with EM micrographs (Figures 6–13) of a somewhat smaller form from Rietvlei Dam, a reservoir situated approximately 40 km S.E. of the Pretoria Salt Pan, suggested a very close relationship between them, size and striae density being the most apparent differentiating characters.

Striae counts of small centric diatoms are troublesome since the small diameter of the valves can result in an overestimation of the number of striae in 10 μm. To overcome this problem our counts were calculated from a table compiled by Dr Gary B. Collins, Cincinnati, U.S.A. (personal communication; *cf.* Collins & Groetsch 1981) from which striae/costae counts for centric diatoms with diameters less than 15 μm can be estimated.

Apart from an appreciable difference in diameter between the two forms, there is also a marked disparity in their striae counts, the larger specimens from sample B9 having 9–10 striae in 10 μm, while the smaller Rietvlei Dam examples had 15–18 striae in 10 μm. This difference may not have real significance since recent studies by Theriot & Stoermer (1981) and Mizuno (1982) have indicated that increases in striae density accompany decreases in valve diameter. It is therefore possible that these examples represent two distinct size populations of the same taxon.

When considering the identity of these two forms our initial impression was that both have a close affinity to *Stephanodiscus minutulus* (Kützing) Round (1981, 462, figures 19–24). However, certain structural differences in the Rietvlei Dam specimens as observed with the EM, led the senior author to contact Mrs H. Håkansson (Lund, Sweden) for her opinion. She suggested that our specimens are not *S. minutulus* but probably belong to the genus *Cyclostephanos* Round (1982, 326). We examined this possibility and agree with her. To date only three species have been assigned to the genus *Cyclostephanos*, viz. *C. dubius* (Fricke) Round (1982), *C. novae zeelandiae* (Cleve) Round (1982) and *C. damasii* (Hustedt) Stoermer & Håkansson (1983). The Rietvlei Dam form appears to be intermediate between *C. dubius* and *C. damasii*, but we hesitate to describe it as a new species until more detailed studies can be conducted. To highlight the differences between our *Cyclostephanos* from Rietvlei Dam and the species mentioned above, we present a description of our taxon based on the EM micrographs (Figures 6–13).

Valves rather small, convex or concave at the centre (Figures 8–11), with a narrow mantle. Striae fascicles multiseriate (2–4 rows of areolae) near the valve margin with *ca.* 50–60 areolae in 10 μm, and uniseriate towards the valve centre where some irregular areolation occurs. The fine structure of the areolae is seen in Figure 7. Interfascicles (costae) distinct, each with a well-developed spine (Sp — Figures 9, 10, 12) near the valve margin where the interfascicles pass over into the mantle, the resulting intercalated mantle striae fascicles (MSF — Figures 9–12) therefore narrower than those on the valve face and possessing only 1–2 short rows of areolae (Figure 12). Internally, there appear to be numerous very short ribs (R) along the valve mantle which seem to radiate from the interfascicles (Figure 13 — rather poor enlargement). The external openings of the marginal strutted processes (MSP — Figures 9, 10, 12) are present in the valve mantle below the marginal spine of every 4th or 5th interfascicle (in the B9 examples, Figures 1 & 5, these openings occur on every 2nd or 4th interfascicle). Internally (Figures 11, 13) each marginal strutted process resembles a short tubule and is flanked by two lateral 'arcs' (A — Figure 13; *cf.* Round 1982). A single strutted process is present near the centre of the valve (CSP — Figures 6, 7, 11).

Although we have no concrete evidence to link the Rietvlei Dam specimens and the forms from the vicinity of the Pretoria Salt Pan, we have provisionally accepted them as one taxon. The larger forms are therefore also placed under the name *Cyclostephanos* sp.

Cymbella aspera (Ehrenberg) Peragallo (Figures 15–18)

Patrick & Reimer 1975, 53, plate 10, figure 2.
Length 90,0–145,0 μm, breadth 20,0–26,5 μm. Transapical striae 7–8 in 10 μm near the centre but denser at the poles, 10–14 in 10μm. The striae are punctate with 10–14 puncta in 10 μm.

Identification of this taxon as *C. aspera* is supported by the work of Krammer (1982a, 29, plates 1058–1065) who richly illustrated this species. Particular note should be taken of Figure 15 showing the external view of a valve pole with the terminal fissure of the raphe and apical pore field (APF) visible, as it corresponds almost exactly with Krammer's illustrations. Figure 16 illustrates the internal view of a valve pole showing clearly the apical pore field and the internal raphe fissure running along the axial rib and terminating in a helictoglossa. The rather characteristic striae structure as observed on the inside of the valve is illustrated in Figures 17 & 18. The striae are relatively narrow and are separated by broad interstriae. Internally, each stria consists of a transapically aligned groove which is furnished with struts and perforated by circular areolae (Figure 18).

Several specimens were observed in sample B2.

Cymbella kolbei Hustedt

Hustedt 1949a, 46, plate 1, figures 20–26.
Schoeman 1973, 56.
Length 20,0–22,5 μm, breadth 6,0 μm. Transapical striae about 12 in 10 μm near the centre but denser at the poles, 17–19 in 10 μm. An isolated stigma is present in the central area above the centremost ventral stria.

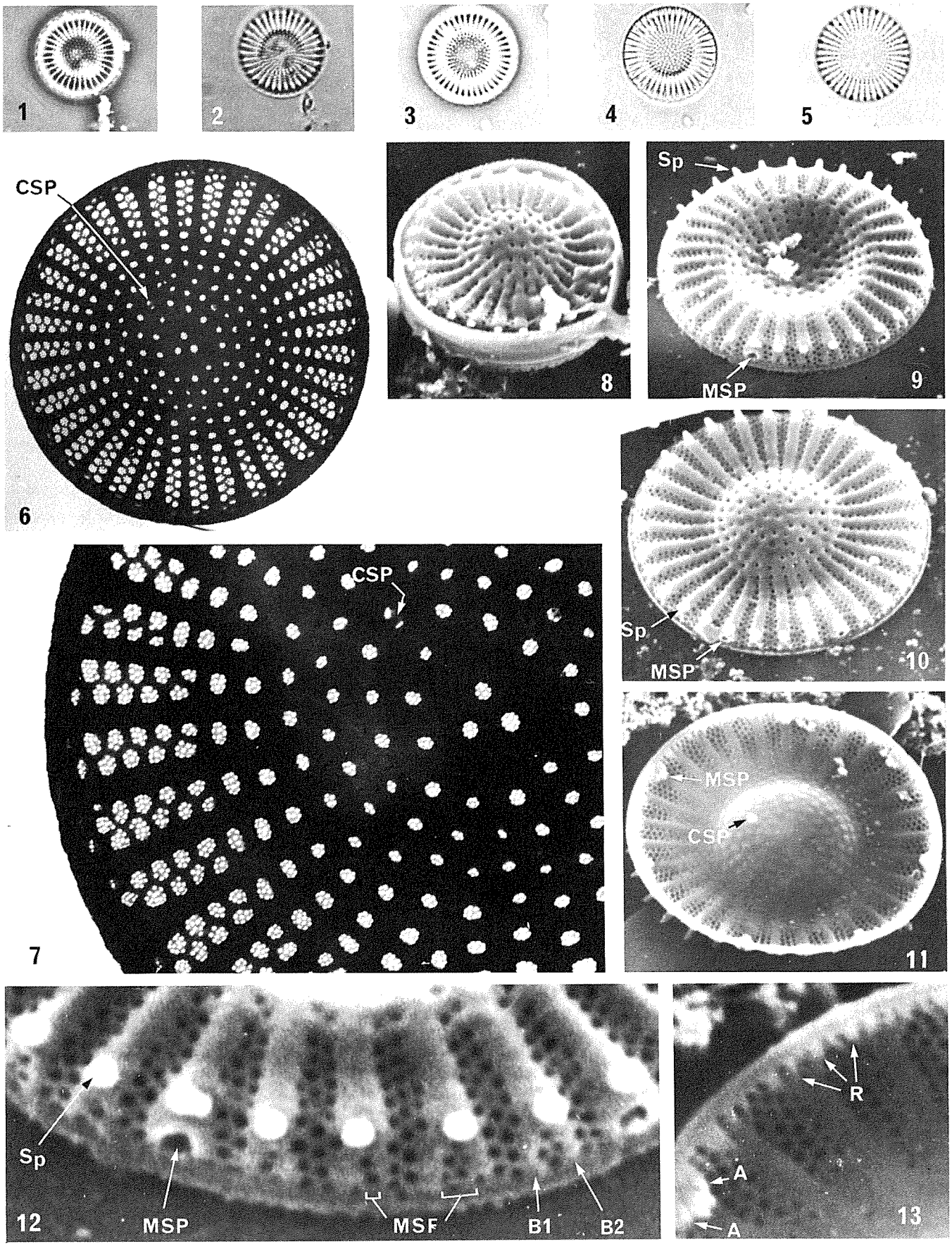

Figures 1–13. Figures 1–5 *Cyclostephanos* sp., sample B9 (×1 500). **1, 2.** Same specimen. **3–5.** Same specimen. **Figures 6–13** *Cyclostephanos* sp., Rietvlei Dam. **6.** TEM, whole valve (×10 500). **7.** TEM, part of valve in 6 enlarged to show structure of striae fascicles (×26 500). **8–10.** SEM, external views of three valves. Note position of marginal spines (Sp) and openings of marginal strutted processes (MSP) (×9 000). **11.** SEM, internal view of whole valve showing both marginal (MSP) and central (CSP) strutted processes (×9 000). **12.** Part of valve in 10 enlarged (external view) showing spines (Sp), a marginal strutted process (MSP), mantle striae fascicles (MSF) and branched interfascicles (B1 and B2) on the mantle (×31 000). **13.** Part of valve in 11 enlarged (internal view) showing the short mantle ribs (R) and the two lateral 'arcs' (A) of a marginal strutted process (×27 000). Figures 1, 3. Phase contrast illumination; Figures 2, 4. Oblique illumination; Figure 5. Bright field illumination.

From an examination of the literature it appears that *C. kolbei* is frequently confused with *C. hustedtii* Krasske (1923, 204, figure 11), and it will be necessary to study the type material of both species to clarify the situation. The two species are morphologically very similar and are distinguished most easily by the presence of a single isolated stigma above the central stria on the ventral side in *C. kolbei*. Prior to Hustedt's description of *C. kolbei*, Kolbe & Krieger (1942, 350, plate 3, figures 16–18) identified specimens from Mesopotamia as *C. hustedtii*, although these possessed isolated stigmata. Based on Kolbe & Krieger's (1942) illustrations, Cholnoky (1954, 121, figures 2, 3) also identified forms with an isolated stigma from the Mogol River (Transvaal) as *C. hustedtii*. However, in a subsequent paper Cholnoky (1956, 62) revised his identification of such forms and assigned them to *C. kolbei*, implying at the same time that Kolbe & Krieger's (1942) specimens should also be regarded as *C. kolbei*.

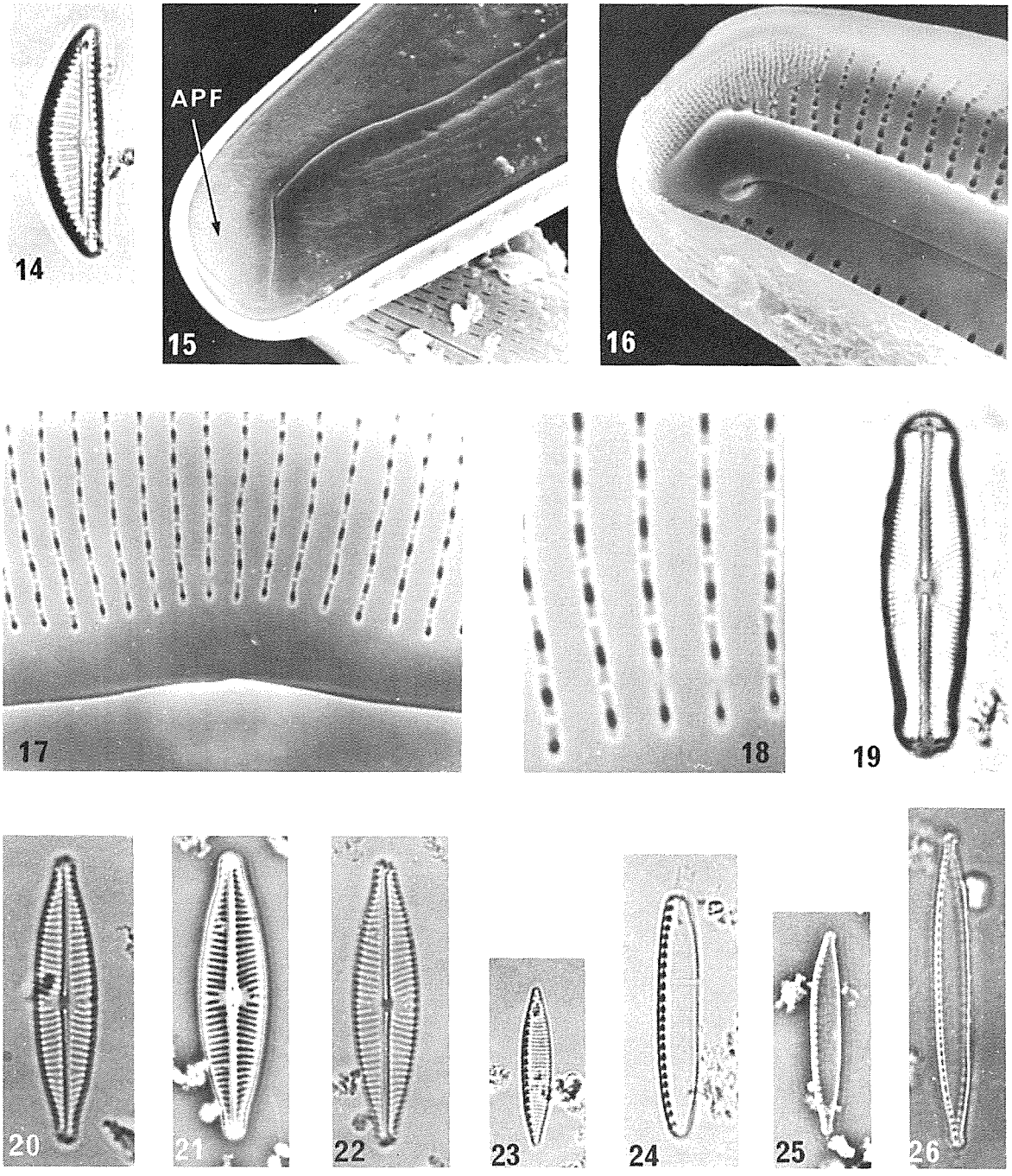

Figures 14–26. Figure 14 *Cymbella minuta* Hilse *ex* Rabenhorst var. *silesiaca* (Bleisch *ex* Rabenhorst) Reimer, LM (×1 500). **Figures 15–18** *Cymbella aspera* (Ehrenberg) Peragallo, SEM. **15.** External view of pole showing the distal end of the raphe including the terminal fissure and the apical pore field (APF) (×5 000). **16.** Internal view of pole showing the raphe fissure terminating in a helictoglossa, and the apical pore field (×5 000). **17.** Internal view showing the structure of the striae at the central nodule (×5 000). **18.** Enlargement of striae on the inner valve surface (×10 000). **Figure 19** *Navicula pupula* Kützing, LM (×1 500). **Figures 20–22** *Navicula cryptocephala* Kützing complex, LM (×1 500). **21, 22.** Same specimen. **Figure 23** *Nitzschia angusteforaminata* Lange-Bertalot, LM (×1 500). **Figure 24** *Nitzschia communis* Rabenhorst, LM (×1 500). **Figures 25, 26** *Nitzschia palea* (Kützing) W. Smith complex, LM (×1 500). Figures 14, 19, 26. Bright field illumination; Figures 20, 22–24. Oblique illumination; Figures 21, 25. Phase contrast illumination.

Recently, Compère (1980, 291, figure 62) described the new form, *C. hustedtii* f. *stigmata*, but neither here nor in subsequent discussions on the form (Compère 1981a, 17, figure 39; 1981b, 155) did he compare his new form with *C. kolbei*. Nevertheless, Compère equated both Cholnoky's (1954) and Kolbe & Krieger's (1942) forms with his f. *stigmata*. Until clarity with respect to these three taxa has been obtained, we elect to retain the name *C. kolbei* for our specimens containing an isolated stigma.
Only 2 valves were observed in sample B8.

Cymbella minuta Hilse *ex* Rabenhorst var. *silesiaca* (Bleisch *ex* Rabenhorst) Reimer (Figure 14)

Patrick & Reimer 1975, 49, plate 8, figures 7–10.
Length 24,0 μm, breadth 6,1 μm. Transapical striae (dorsal) 10 in 10 μm near the centre and up to 16 in 10 μm at the poles. Transapical striae (ventral) 11 in 10 μm near the centre and up to 18 in 10 μm at the poles. Lineae (areolae) 28–30 in 10 μm. The central dorsal striae terminate with a stigma.

Superficially, the specimen illustrated here (Figure 14) resembles *C. ventricosa* Kützing = *C. minuta* Hilse *ex* Rabenhorst (Patrick & Reimer 1975, 47). However, the striae density of 10–11 in 10 μm is less than the 14–16 and 12–18 in 10 μm reported by Patrick & Reimer (1975) and Hustedt (1930) respectively. The lineae per 10 μm in our specimen are also fewer than those recorded for *C. minuta*. Except for a slightly narrower breadth, our specimen fits the description of *C. minuta* var. *silesiaca* rather well and we therefore assign our specimen to this taxon.
A single valve was observed in sample B2.

Gomphonema gracile Ehrenberg — *G. parvulum* (Kützing) Kützing complex (Figures 27–48)

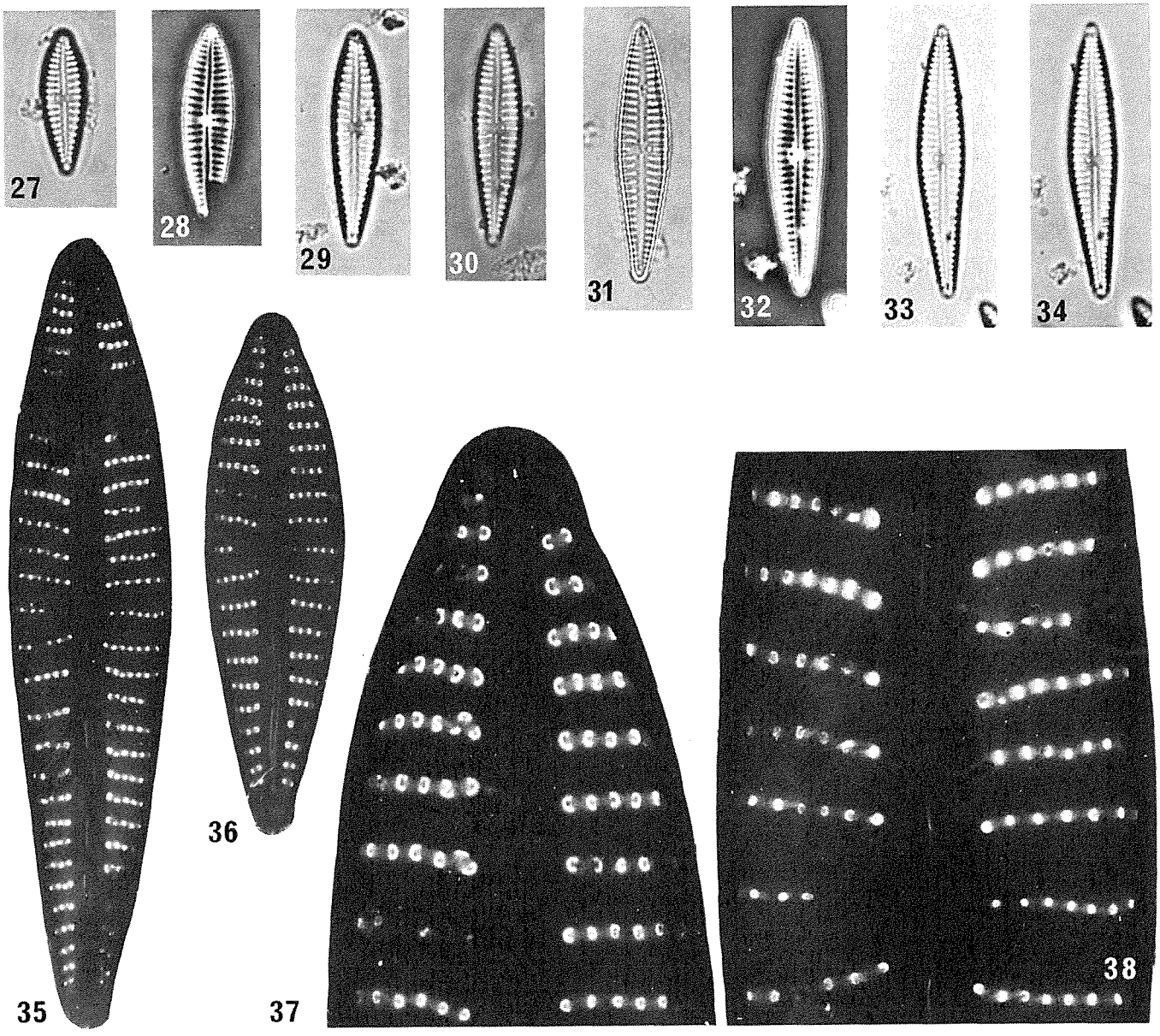

Figures 27–38. Figures 27–34 *Gomphonema gracile* Ehrenberg — *G. parvulum* (Kützing) Kützing complex, LM (×1 500), sample B5. **32–34.** Same valve, different methods of illumination. **Figures 35–38** *G. gracile* Ehrenberg — *G. parvulum* (Kützing) Kützing complex, TEM, sample B5. **35.** Complete valve (×5 400) with centre enlarged in **38** (×14 700) to show the striae structure. **36.** Another complete valve (×5 400) with a part enlarged in **37** (×15 000) to illustrate the striae structure. Figures 27, 30, 31, 33. Bright field illumination; Figures 28, 32. Phase contrast illumination; Figures 29, 34. Oblique illumination.

Sample B5, Figures 27–43. Length 15,0–29,0 μm, breadth 4,5–5,3 μm. Transapical striae 12–16 in 10 μm near the centre and denser, 18–20 in 10 μm at the poles. In TEM the striae are punctate, 37–46 pores in 10 μm.

Sample B2, Figures 44–48. Length 25,0–50,0 μm, breadth 5,5–8,2 μm. Transapical striae 12–16 in 10 μm near the centre and up to 20 in 10 μm at the poles. In TEM the striae are punctate, 35–40 pores in 10 μm.

In this complex we have grouped together a number of forms, which, depending on various interpretations, have been identified by others as either *G. parvulum* or *G. gracile*. Consequently, the identity of the specimens allotted to this complex has been difficult to determine. In sample B5 we have a number of forms (Figures 27–34) which appear to constitute an intergrading series. On the basis of valve shape (*cf.* Lowe 1972; Dawson 1973, 415; Patrick & Reimer 1975, 122 & 131 and Germain 1981, 308 & 310), this series passes from *G. parvulum*-shaped valves (Figures 27–30) to *G. gracile*-shaped valves (Figures 31–34).

According to a table (Dawson 1973, 415) summarizing characters other than dimensions and valve shape, found in various *Gomphonema* species, *G. parvulum* has radial striae whereas *G. gracile* has transverse or parallel striae. In the sample B5 series, all the specimens had radial striae, although sometimes the striae near the centre of the valve became more or less parallel. The table also indicates that the raphe in both *G. gracile* and *G. parvulum* is straight. It is, however, difficult to know what Dawson means by straight, since in an earlier paper on *G. parvulum* (Dawson 1972) EM micrographs show the raphe branches to be slightly curved, rather than straight or undulate. All the specimens from sample B5 had similar, slightly curved raphe branches. Finally, Dawson's table states that *G. gracile* has a mucilage pore area at both apical and basal poles. SEM studies of specimens from sample B5 (Figures 39, 40, 42, 43) have shown that in this series a mucilage pore area (MPA) is present only at the basal pole. Although this table does not help to identify the specimens from sample B5 clearly, it seems to support their identification as *G. parvulum* more strongly.

In TEM there appears to be no difference in the striae structure between the *G. parvulum*-like forms (Figures 36, 37) and the *G. gracile*-like forms (Figures 35, 38). In both forms the apertures to the areolae are reniform, horseshoe-shaped, E- or S-shaped slits. This characteristic structure has

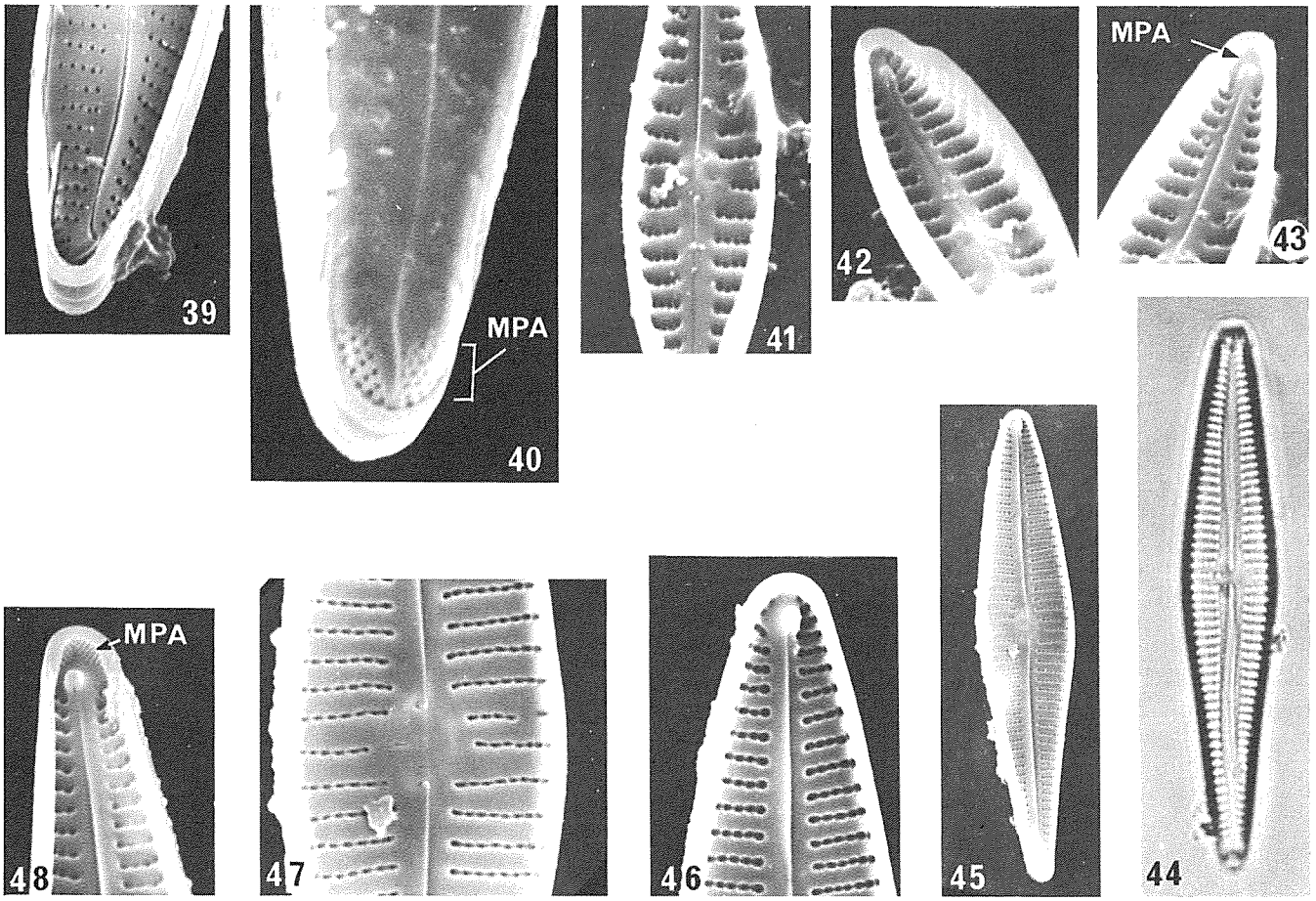

Figures 39–48. Figures 39–43 *Gomphonema gracile* Ehrenberg — *G. parvulum* (Kützing) Kützing complex, SEM, sample B5. **39.** External view, apical pole without mucilage pore area (×6 000). **40.** External view, basal pole with mucilage pore area (MPA) (×12 000). **41.** Internal view showing central striae and isolated stigma (×6 000). **42.** Internal view of same valve showing apical pole (×6 000). Note absence of mucilage pore area. **43.** Internal view of same valve but showing the basal pole with its mucilage pore area (MPA) (×6 000). **Figure 44** *G. gracile* Ehrenberg — *G. parvulum* (Kützing) Kützing complex, LM (oblique illumination), specimen from sample B2 (×1 500). **Figures 45–48** *G. gracile* Ehrenberg — *G. parvulum* (Kützing) Kützing complex, SEM internal views of another specimen from sample B2. **45.** Whole valve (×2 000). **46.** Apical pole (without mucilage pore area) of valve in 45 enlarged (×6 000). **47.** Centre of valve in 45 enlarged (×6 000). **48.** Basal pole of valve in 45 enlarged and showing the mucilage pore area (MPA) (×6 000).

been observed in *G. parvulum* by Helmcke & Krieger (1953, plate 79), Okuno (1974, plate 908), Dawson (1972, figures 9–11) and Lange-Bertalot (1978, plate 12, figure 4). Mann (1981, figure 21), however, has shown the same striae structure in *G. gracile*.

Figures 44–48 depict another form of *Gomphonema* from sample B2, which has been associated with *G. gracile*. These valves were larger than the specimens from sample B5, but in valve shape and structure this form agreed with Gasse's (1980, plate 48, figures 35–37) interpretation of *G. gracile*. In some respects it conforms to characters attributable to *G. gracile* in Dawson's (1973, 415) table, but in others it does not. Like the specimens from sample B5 it also has a mucilage pore area only at the basal pole (Figures 46, 48).

Our study of the literature has shown that there are conflicting views on the characters regarded as specific for the identification of *G. gracile* and *G. parvulum*. The variation recorded in our present study emphasizes the problem and clearly points to the need for a revision of these species based on authenticated material.

Navicula cryptocephala Kützing complex (Figures 20–22)

Length 20,5–32,0 μm, breadth 5,5–6,5 μm. Transapical striae 14–16 in 10 μm.

In an earlier paper on the diatoms of the Pretoria Salt Pan vicinity (Schoeman & Ashton 1982b, 30, figures 19–22, 51, 52, 92–94) figures and notes were given on forms regarded as being representative of the true *N. cryptocephala*. The forms figured here (Figures 20–22) appear to be intermediate between *N. cryptocephala* and the var. *veneta* (Kützing) Rabenhorst (= *N. veneta* Kützing, *cf.* Lange-Bertalot 1979, 209, figures 40–46, 71, 72). Our forms also show some resemblance to the var. *lancettula* Schumann *sensu* Germain (1981, plate 72, figure 6). However, a study of the literature showed that *N. cryptocephala* is extremely variable from a morphological point of view. For this reason no further attempt has been made to identify our forms with any specific variety.

These forms have been recorded from samples B2 and B5.

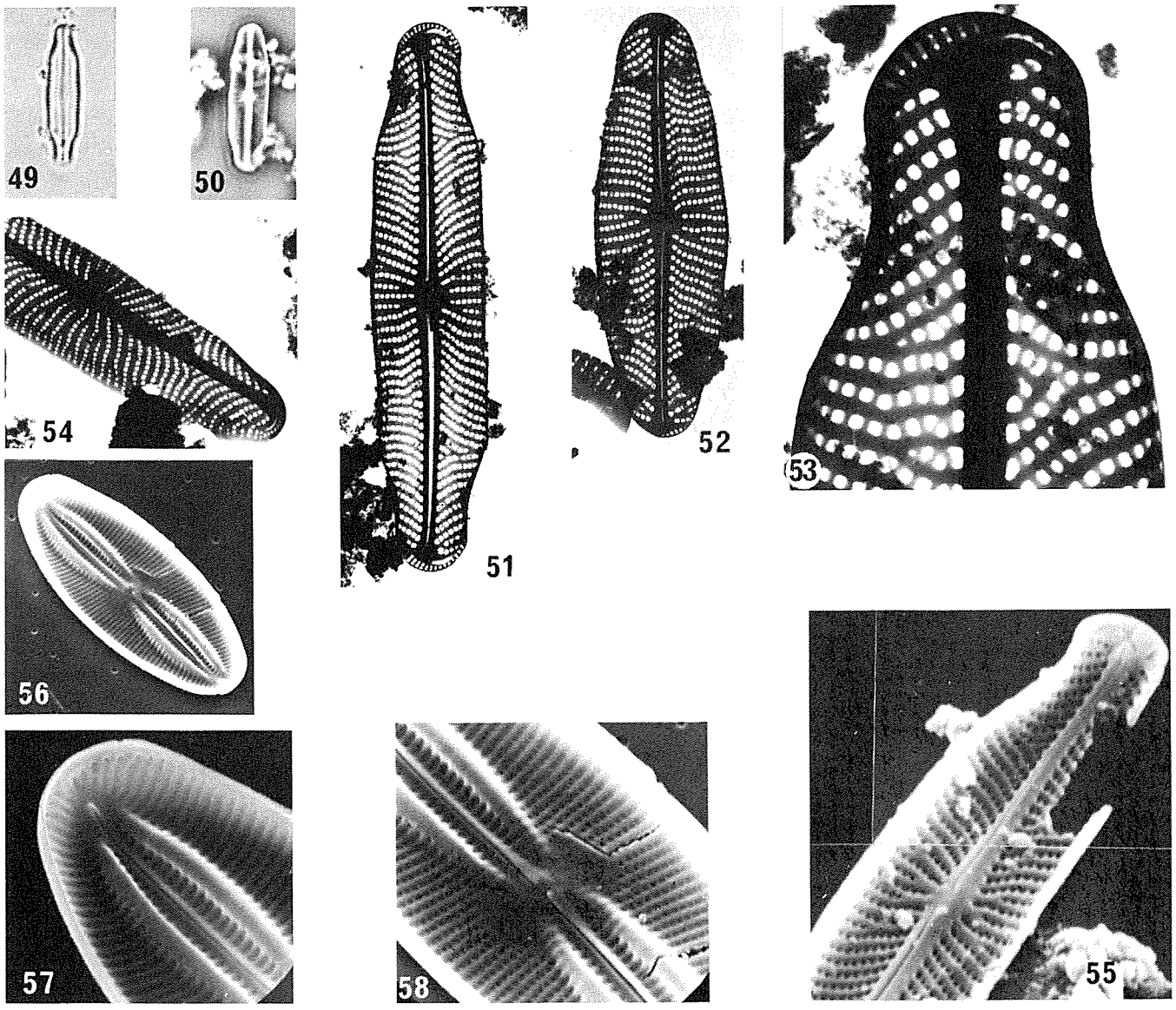

Figures 49–58. Figures 49, 50 *Navicula maillardii* Germain, LM (×1 500). **Figures 51–54** *Navicula maillardii* Germain, TEM. **51, 52, 54.** (×5 400). **53.** A pole enlarged (×18 000). **Figure 55** *Navicula maillardii* Germain, SEM, internal view (×10 000). **Figures 56–58** *Navicula pygmaea* Kützing, SEM, internal views. **56.** Whole valve (×2 400). **57.** Pole enlarged (×6 000). **58.** Centre of valve enlarged (×6 000). Figure 49. Oblique illumination; Figure 50. Phase contrast illumination.

Navicula maillardii Germain (Figures 49–55)

Germain 1982, 107, figures 19–23.
Length 12,0–16,0 μm, breadth 3,0–4,0 μm. Transapical striae 30–36 in 10μm with 56–66 puncta in 10 μm.

The specimens illustrated in Figures 49–55, although showing some resemblance to *N. bryophila* J. Boye Petersen (*cf.* Hustedt 1961–66, 91, figure 1237; Ando 1979, figures 42–49), have been identified as *N. maillardii* Germain (1982, 107). Our specimens displayed a wider variation in valvar shape than was noted by Germain (l.c.). In this regard the valves usually possess subcapitate poles (Figures 49, 51, 53) but may also be broadly rostrate (Figures 50, 52). Most of our samples have weakly tri-undulate valve margins (Figures 49–51) whereas others only possess a central inflation (Figure 52). Unfortunately we have not been able to observe the fine structure of the puncta reported by Germain (1982, figure 23) since the acid cleaning process destroyed it. Observed with the SEM (Figure 55), the areolae of the striae open internally into radially aligned transapical grooves. This micrograph (Figure 55) also shows the internal raphe fissures running along a raised axial rib and terminating in small helictoglossae at the poles. The strongly curved terminal fissures are clearly seen in TEM (Figures 51, 53). This species represented 15,4% of the diatom association in sample B1.

Navicula sp. [*affin. radiosa* Kützing] (Figures 59–61)

Length 51,0–59,0 μm, width 7,0–8,5 μm. Transapical striae 13–14 in 10 μm off centre and up to 17 in 10 μm at the poles. In TEM the striae consist of a single row of areolae, 35–39 in 10 μm.

We have not been able to identify with any certainty the specimens illustrated in Figures 59 & 60. As regards general valvar shape and structure they resemble *N. radiosa* but differ from it in being narrower and possessing 13–14 transapical striae in 10 μm instead of the 10–12 in 10 μm recorded in the literature (Hustedt 1930, 299, figure 513; Patrick & Reimer 1966, 509, plate 48, figure 15). Our examples also show some resemblance to *N. radiosa* var. *tenella* (Brébisson *ex* Kützing) Grunow (Hustedt 1930, 299; Patrick & Reimer 1966, 510, plate 48, figure 17) but differ from this variety in the structure of the central area and the density of the striation. Our specimens have fewer striae in 10 μm than the 15–18 in 10 μm recorded in the literature (Hustedt l.c.; Patrick & Reimer l.c.). However, in a more recent publication Germain (1981, 182, plate 70, figures 1–8) maintains that *N. radiosa* may be only 7 μm broad and that the var. *tenella* has about 14 striae in 10 μm (Germain 1981, 184, plate 70, figures 9–12). Taking this information into consideration it appears that our specimens are intermediate between *N. radiosa* and its variety, var. *tenella*. In TEM (Figure 61) the striae structure, a single row of apically elongated areolae, is very similar to that observed in *N. radiosa* by Helmcke & Krieger (1954, plate 172).
This species was recorded from sample B2.

Navicula schroeteri Meister (Figure 71)

Meister 1932, 38, figure 100.
Hustedt 1937–38, 267, plate 18, figure 16.
Germain 1981, 195, plate 74, figures 1–6.
Length 30,0–38,0 μm, breadth 6,5–7,0 μm. Transapical striae 13–15 in 10 μm.

Although Meister (1932, 38) gave 12 striae in 10 μm in his original description of this species, striae counts of up to 15 in 10 μm have been recorded in the literature (Hustedt 1937–38; Foged 1980; Compère 1981a; Germain 1981). In the specimens observed here the transapical striae were usually strongly radial, but in some examples the polar striae were less radial or even parallel (Figure 71). Specimens having fewer radial polar striae have also been illustrated by Foged (1971, plate 11, figure 16) and Compère (1981a, figure 118). In TEM (Figure 71) the striae are shown to consist of a single row of apically elongated areolae, 22–28 in 10 μm. Similarly, Foged (1971, 306) observed 22–24 areolae in a specimen with 14 striae in 10 μm.
Only a few examples of this species were observed in sample B2.

Navicula towutiensis Cholnoky (Figures 66–70)

Cholnoky 1963, 245, plate 8, figure 24.
Archibald 1983, 221, figure 349.
Length 32,5–36,5 μm, breadth 7,3–8,2 μm. Transapical striae 12–14 in 10 μm near the centre and slightly denser at the poles, 13–15 in 10 μm.

Our specimens fit very closely the amended description and dimensions given by Archibald (1983). The only difference encountered was in regard to the number of areolae in 10 μm, 24–27(29) in our examples compared with a count of 22–24 recorded by Archibald (1983). In TEM (Figure 70) the striae are seen to consist of a single row of somewhat apically elongated areolae.
This was a rare species in sample B5.

Navicula zanonii Hustedt (Figures 62–65)

Hustedt 1949b, 92, plate 5, figures 1–5.
Length 35,0 μm, breadth about 7 μm. Transapical striae 14–15 in 10 μm, radial at the centre and convergent at the poles. Each stria is composed of a single row of areolae, 36–40 in 10 μm.

Based on valve shape, dimensions and structure of the striae and central area, the single specimen observed during the SEM examination of sample B1 (Figure 62) has been identified as *N. zanonii*. This specimen also agrees well with an LM photograph of an example from Lake Edward (the type locality — slide BRM 244/53 in the Hustedt collection) taken by Mayama & Kobayasi (1982, 92, figure 64). Gasse (1980, 71, plate 41, figures 7–11, 13; plate 46, figures 1–8) has illustrated some of the variations in this species from Ethiopia. The internal views of our specimen (Figures 62–65) are very similar to those illustrated by her (Gasse 1980, plate 46, figures 1–5). These views also show that the striae consist of a single row of areolae sunk in a linear groove or depression, particularly clearly seen in Figure 64. Viewed from the inside, the shape and structure of the central nodule (Figures 64, 65) are very similar to those depicted by Krammer (1982b, figure 4) for *N. radiosa* (*cf.* also Cox 1977, figure 27). Here we see that the inner raphe fissure is displaced to one side along a raised axial rib (Figures 62, 65). The proximal ends open fairly close to each other on the central nodule (Figures 64, 65) while the distal ends terminate in helictoglossae (Figure 63).

Nitzschia amphibia Grunow (Figures 72–86)

Hustedt 1930, 414, figure 793.

Germain 1981, 358, plate 135, figures 32–37.
Length 11,0–21,5 μm, breadth 3,5–4,0 μm. Transapical striae 16–18 in 10 μm with 20–27 puncta in 10 μm. Fibulae 7,5–8,5 in 10 μm.

Our TEM examination of this species has shown that in all specimens the raphe fissure is interrupted at the centre of the valve (Figures 76, 77; *cf.* Helmcke & Krieger 1953, plate 85). This interruption may be seen in SEM as a small central nodule on the external valve surface (CN — Figures 81, 82), which is also visible through the usually enlarged central portula (CN — Figures 85, 86). Since the specimens examined in this study are relatively small, it refutes

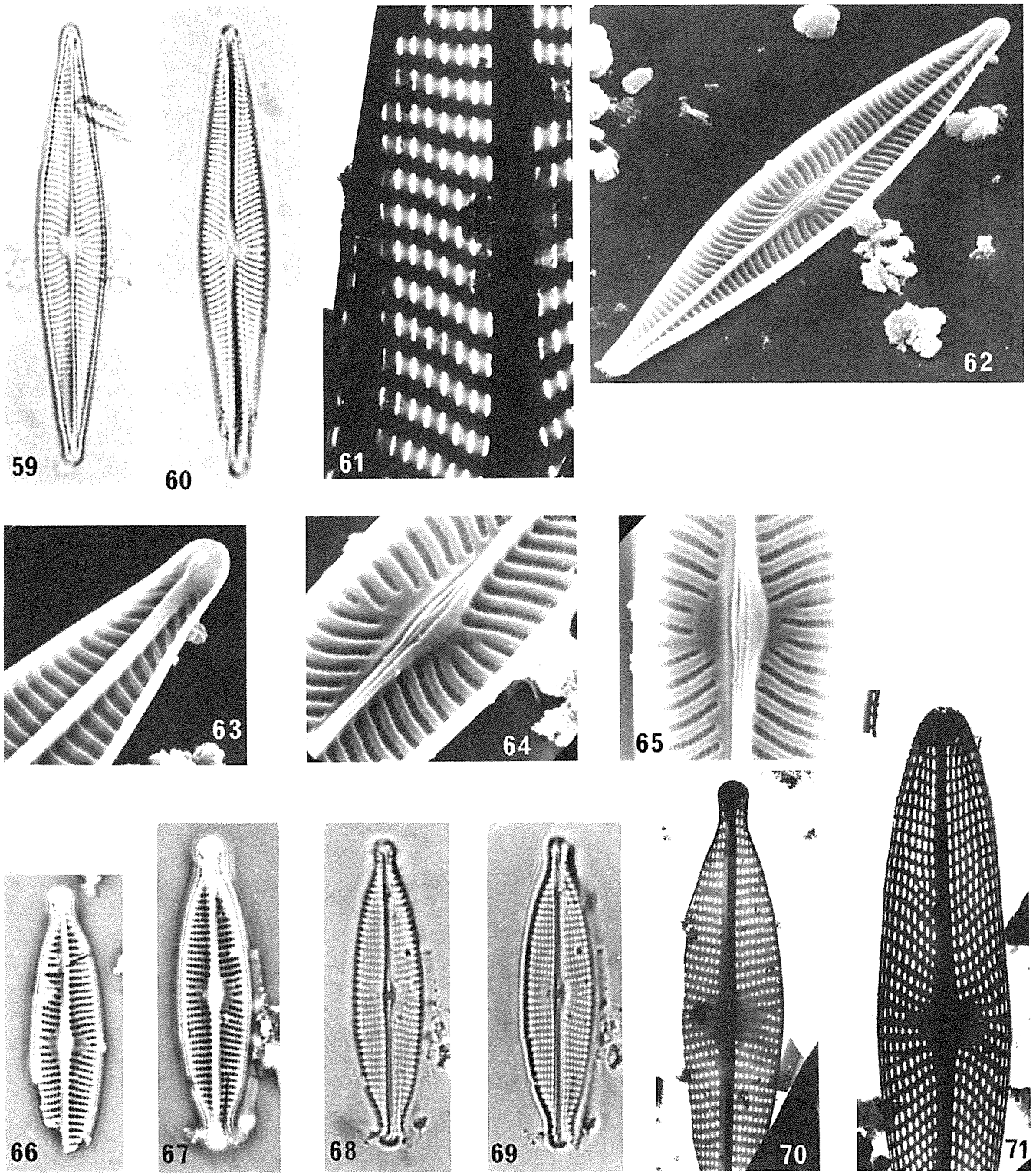

Figures 59–71 Figures 59, 60 *Navicula* sp. [affin. *radiosa* Kützing], LM (×1 500). **Figure 61** *Navicula* sp. [affin. *radiosa* Kützing], TEM. Enlargement to show structure of the striae (×10 000). **Figures 62–65** *Navicula zanonii* Hustedt, SEM, internal views of the same valve. **62.** Whole valve (×3 000). **63.** Pole enlarged showing axial rib and small helictoglossa (×6 000). **64 & 65.** Centre enlarged, tilted in 64 and lying flat in 65. Note the structure of the striae and central nodule with the proximal ends of the inner raphe fissures (×6 000). **Figures 66–69** *Navicula towutiensis* Cholnoky, LM (×1 500). **67–69.** Same specimen. **Figure 70** *Navicula towutiensis* Cholnoky, TEM (×2 500). **Figure 71** *Navicula schroeteri* Meister, TEM (×3 600). Figures 59, 60. Bright field illumination; Figures 66, 67. Phase contrast illumination; Figures 68, 69. Oblique illumination.

Hustedt's (1937–38, 476) statement that a central nodule is only present in the larger examples (*cf.* Lange-Bertalot 1977, 260). Distally, the raphe fissure ends in a somewhat ornately hooked terminal fissure (TF—Figure 83). Externally

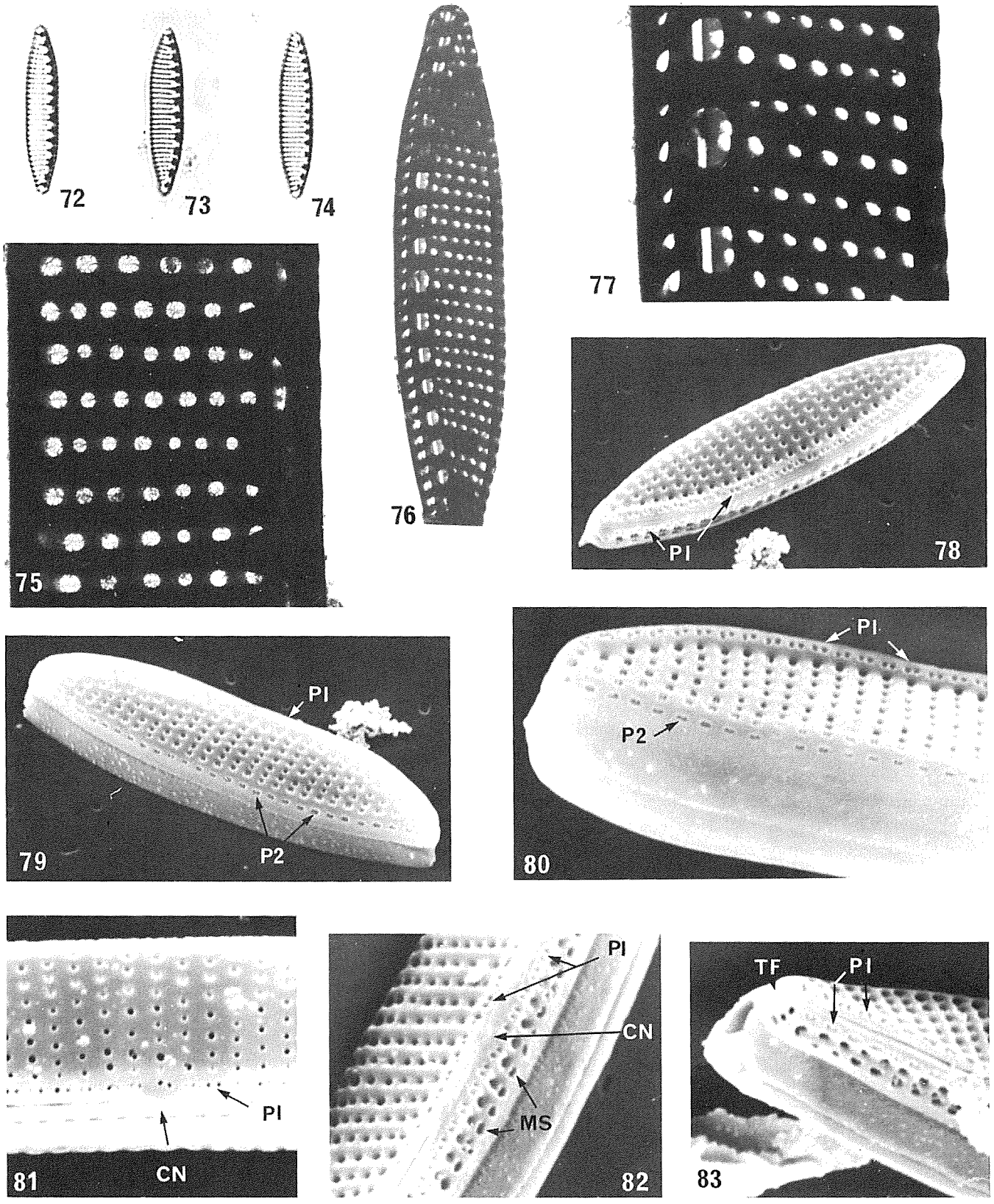

Figures 72–83 **Figures 72–74** *Nitzschia amphibia* Grunow, LM (×1 500). **Figures 75–77** *Nitzschia amphibia* Grunow, TEM. **75.** Portion of valve enlarged to show presence of a velum in each areola (×14 500). **76.** Whole valve showing raphe canal (×5 400). **77.** Centre of specimen in 76 enlarged to show interruption of raphe fissure by central nodule (×15 000). **Figures 78–83** *Nitzschia amphibia* Grunow, SEM, external views. **78, 79.** Whole valve, same specimen but turned through 210° in 79 (×6 000). **80.** Enlargement of one half of a valve showing both large (P1) and small (P2) pairs of pores (×9 000). **81.** Enlargement of centre of valve showing a small central nodule (CN) and proximal ends of raphe fissures (×9 000). **82.** Centre of another valve with central nodule (CN), two rows of large pores (P1) in pairs and mantle striae (MS) (×9 000). **83.** Pole of a valve showing curved terminal fissure (TF) (×9 000). Figures 72, 74. Bright field illumination; Figure 73. Oblique illumination.

on either side of the raphe fissure there is a row of double pores (P1 — Figures 80–82). Each pair of pores lies opposite a stria, be it a valvar or mantle stria. Along the opposite margin of the valve there is a similar arrangement with a row of paired pores (P2 — Figures 79, 80) on either side of a marginal costa. These pores (P2) are, however, slightly smaller than the paired pores associated with the raphe. On the inside of the valve the fibulae (F — Figure 84) are conspicuous and vary in width so that they span from one to three interstriae with which they are fused (Figures 84–86; *cf.* Lang & Pierre 1974, plate 3, figure 2; Lange-Bertalot 1977, plate 10, figure 4). Because of this the fibulae in LM often assume a U- or M-shaped appearance, depending on the number of projections per fibula that fuse with the interstriae (*cf.* Germain 1981, plate 135, figures 32–37). This arrangement also regulates the size and spacing of the portulae. The transapical striae consist of a single row of circular areolae in which each areola is occluded by a velum (Figure 75). This is in agreement with the observations of Helmcke & Krieger (1953, plate 85), Lange-Bertalot & Simonsen (1978, plate 22, figure 295) and Germain (1981, plate 163, figure 2). The striae lie in transapical grooves separated by costa-like interstriae (Figures 80, 82, 84, 86). Mantle striae (MS — Figure 82) are present only on the raphe side of the valve, while the mantle on the opposite side remains structureless apart from the row of paired pores mentioned above (Figure 80).
N. amphibia is the dominant diatom species in sample B5 but is also present in samples B2 and B6.

Nitzschia angusteforaminata Lange-Bertalot (Figure 23)

Lange-Bertalot 1980a, 43, figures 44–51, 127–132.
Length 16,0–17,5 μm, breadth about 3,0 μm. Transapical striae about 24 in 10 μm. Fibulae about 12 in 10 μm, the two central ones not more widely spaced than the others.

In many aspects, the forms observed here resemble taxa in the *N. frustulum* complex (*sensu* Lange-Bertalot & Simonsen 1978). However, owing to the presence of equidistant fibulae at the centre and close agreement with Lange-Bertalot's (1980a) description, we prefer to identify them as *N. angusteforaminata*.
This is a rare species in sample B8.

Nitzschia frustulum (Kützing) Grunow

Lange-Bertalot 1977, 262, plate 2, figures 6–8, plate 9, figures 3,4.
Lange-Bertalot & Simonsen 1978, 23, figures 1–39, 292, 293.
Archibald 1983, 256.
Length 10,0–40,0 μm, breadth 2,5–3,2 μm. Transapical striae 24–30 in 10 μm. Fibulae 10–12 in 10 μm, the central two more widely spaced than the rest.

Despite the publications by Lange-Bertalot (1977) and Lange-Bertalot & Simonsen (1978) dealing with the concept of *N. frustulum*, there still appears to be some uncertainty concerning the range of its morphological variability (Gasse 1980, 77–78; Archibald 1983, 256). The dimensions of our specimens and their good agreement with Lange-Bertalot & Simonsen's (1978, 24) description, particularly the greater separation of the two central fibulae, encourages us to identify them as *N. frustulum*. However, care should be exercised when accepting records and data of *N. frustulum* in the literature. A single character, namely the wider separation of the two central fibulae, can in many cases be readily employed to detect a misidentification, provided a suitable illustration of the relevant organism is supplied (e.g. Lewin & Lewin 1960, figures 17–19; Hargraves & Levandowsky 1971, 327, plate 3, figure 26).
N. frustulum is recorded from samples B1 and B2.

Nitzschia palea (Kützing) W. Smith complex (Figures 25, 26)

Length 21,0–44,0 μm, breadth 3,0–4,0 μm. Transapical striae fine, 36+ in 10 μm. Fibulae 12–16 in 10 μm, the central two not more widely spaced than the rest.

Lange-Bertalot (1977, 271, plate 3, figures 17–25) states that *N. palea* is taxonomically the second most complicated species in the genus *Nitzschia*. It appears that the variation within this species is exceedingly large (*cf.* Archibald 1983, 279). Many examples from our samples resemble the var. *debilis* (Kützing) Grunow as described and illustrated by Lange-Bertalot (1980a, 51, figures 9–13) who distinguished it (EM study) from the species on the grounds that it has comparatively larger areolae (Lange-Bertalot 1980a, figures 110–112 and 113, 114). In the present study, however, we decided not to distinguish between the species and its var. *debilis*.
Specimens belonging to the *N. palea* complex were recorded from samples B2, B4, B7–B9.

Rhopalodia gibba (Ehrenberg) O. Müller (Figures 87–93)

Hustedt 1930, 390, figure 740.
Length 72,5–105,0 μm, breadth of valve 9,0–10,5 μm. Primary costae 7–8 in 10 μm. Transapical striae 14–17 in 10 μm. In TEM the striae consist of a double row of puncta, 25–38 in 10 μm.

The identity of the specimens illustrated in Figures 87–93 presents a problem. Based on the general shape of the valves (*cf.* Hustedt 1930) our examples can be identified as *R. gibba*. On the grounds of striae density the striae counts for our specimens (14–17 in 10 μm) are greater than those given by Hustedt (1930, 389 and 390) for both *R. gibba* (12–14 in 10 μm) and *R. parallela* (Grunow) O. Müller (12 in 10 μm), although several recent works have recorded up to 16 striae in 10 μm (Patrick & Reimer 1975, 189; Archibald 1983, 304) and even as high as 20 in 10 μm for *R. gibba* (Germain 1981, 320). However, when striae structure is taken into account we are faced with a problem. Careful examination of our specimens in TEM (Figure 90) and SEM (Figure 93) show that each stria is composed of two rows of puncta arranged either alternately, or opposite each other or both ways in the same stria. According to Patrick & Reimer (1975) and Hustedt (1930) this structure is the chief character distinguishing *R. parallela* from *R. gibba*, the latter possessing only one row of puncta per stria. This introduces a complication since Miller (1971, plate 5:XI, figure 4) and possibly also Gerloff & Helmcke (1977, plate 1003 — striae not very clear) present SEM illustrations of *R. gibba* with striae composed of double rows of pores. We are therefore concerned as to the validity of this diagnostic character. Having scanned the literature it was also clear that no one has studied this particular problem with reference to the type specimens or other authenticated material of these two species. Consequently, at this stage, we prefer to identify our specimens as *R. gibba*.

Figure 91 illustrates the external structure of a portion of a valve as seen with SEM. The raphe fissure of the canal raphe, borne on a keel running along the dorsal margin of the valve face, is clearly visible and ends at the central nodule with a downward deflection of the two branches (*cf.* Gerloff & Helmcke 1977, plates 1000, 1001). The

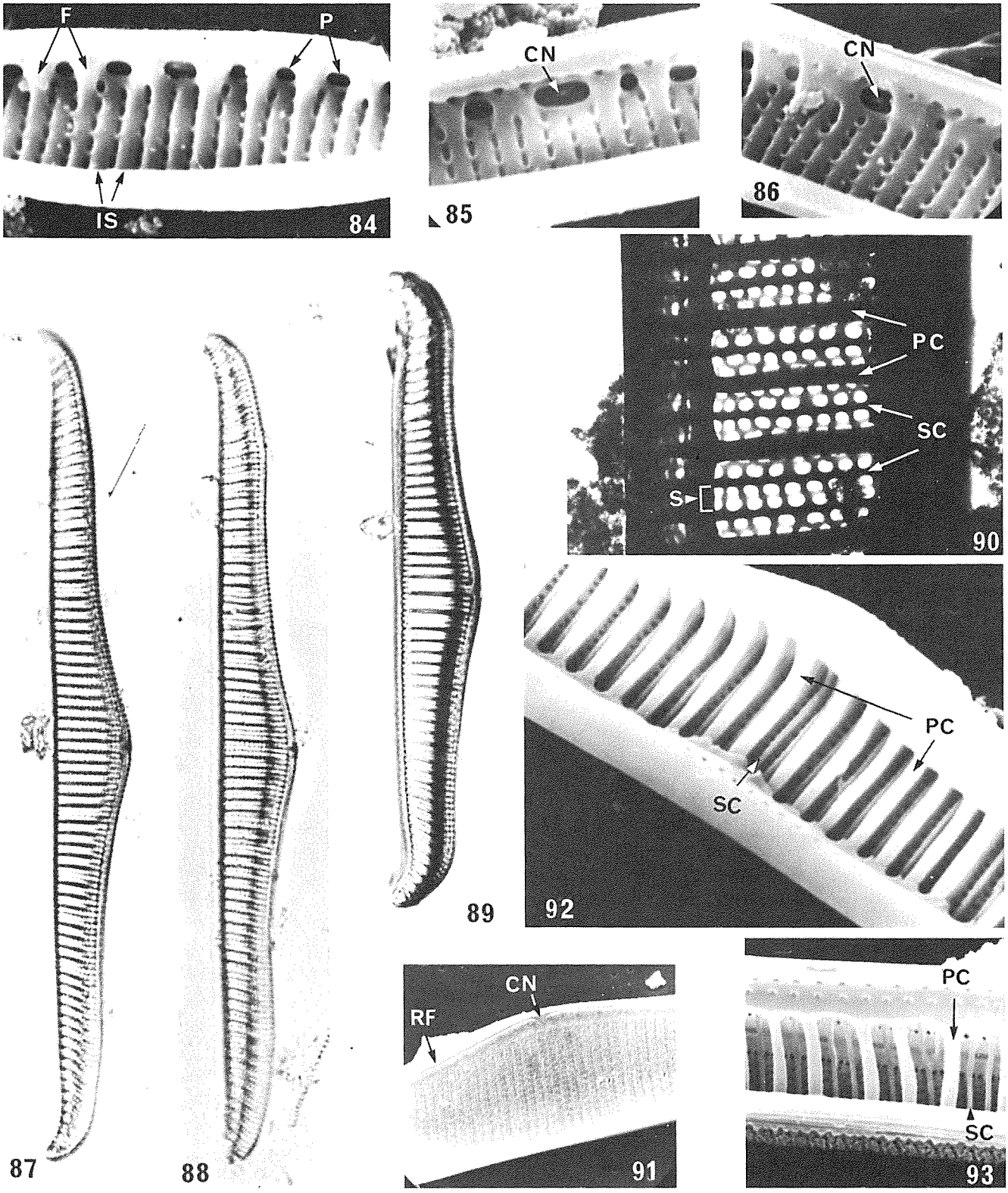

Figures 84–93. Figures 84–86 *Nitzschia amphibia* Grunow, SEM, internal views (×9 000). **84.** Section of valve showing costa-like interstriae (IS), areolae, fibulae (F) and portulae (P). **85.** Centre of a valve with the central nodule (CN) just visible through the enlarged central portula. **86.** Centre of another valve illustrating the structure of the striae and the presence of a central nodule (CN). **Figures 87–89** *Rhopalodia gibba* (Ehrenberg) O. Müller, LM, bright field illumination (×1 500). **Figure 90** *Rhopalodia gibba* (Ehrenberg) O. Müller, TEM. Enlargement of part of valve showing primary costae (PC), secondary costae (SC) and striae (S) each of which consists of a double row of pores (×10 000). **Figure 91** *Rhopalodia gibba* (Ehrenberg) O. Müller, SEM, external view showing central nodule (CN) and raphe fissure (RF) (×3 250). **Figures 92, 93** *Rhopalodia gibba* (Ehrenberg) O. Müller, SEM, internal views of same specimen at different angles of tilt (×6 000). Note the large primary costae (PC) and thinner secondary costae (SC).

internal structure of the valve is more interesting. Figures 92 & 93 show robust transapical primary costae (PC) traversing the valve face and mantle (Figure 92), while much thinner secondary costae (SC — Figures 90, 92, 93), lying between the primary costae, separate the striae composed of double rows of areolae. The canal raphe communicates internally with the cell contents by means of a series of openings or portulae which are faintly visible in Figure 93.
R. gibba was observed in samples B2, B4, B6–B9. It represented the dominant diatom species in samples B7 and B8.

Synedra rumpens Kützing

Hustedt 1931–59, 207, figures 697a, b.
Lange-Bertalot (1980b, 729, 747) recently transferred this species to the genus *Fragilaria* as *F. capucina* Desmazières. However, we prefer to maintain the name *S. rumpens*.
This is a rare species in sample B4.

Synedra ulna (Nitzsch) Ehrenberg complex (Figures 96, 97)

Length 171,0–350,0 μm, breadth 3,8–5,0 μm. Transapical striae 9,5–11 in 10 μm.

While undertaking the initial LM examination of the samples we experienced no difficulty in identifying these specimens as belonging to the *S. ulna* complex and particularly to var. *danica* (Kützing) Grunow (*cf.* Hustedt 1931–59, 200, figure 691A, f) in which valves are less than 5,0 μm broad.

Nevertheless, during an EM examination of sample B2 containing examples of these forms, some interesting features concerning striae structure were observed. Figure 96 shows a valve in which the striae have a double row of pores arranged alternately. In contrast, however, the valve shown in Figure 97 displayed striae with a wide variation in structure from some composed of a single row of pores to others with a double row of alternating pores including

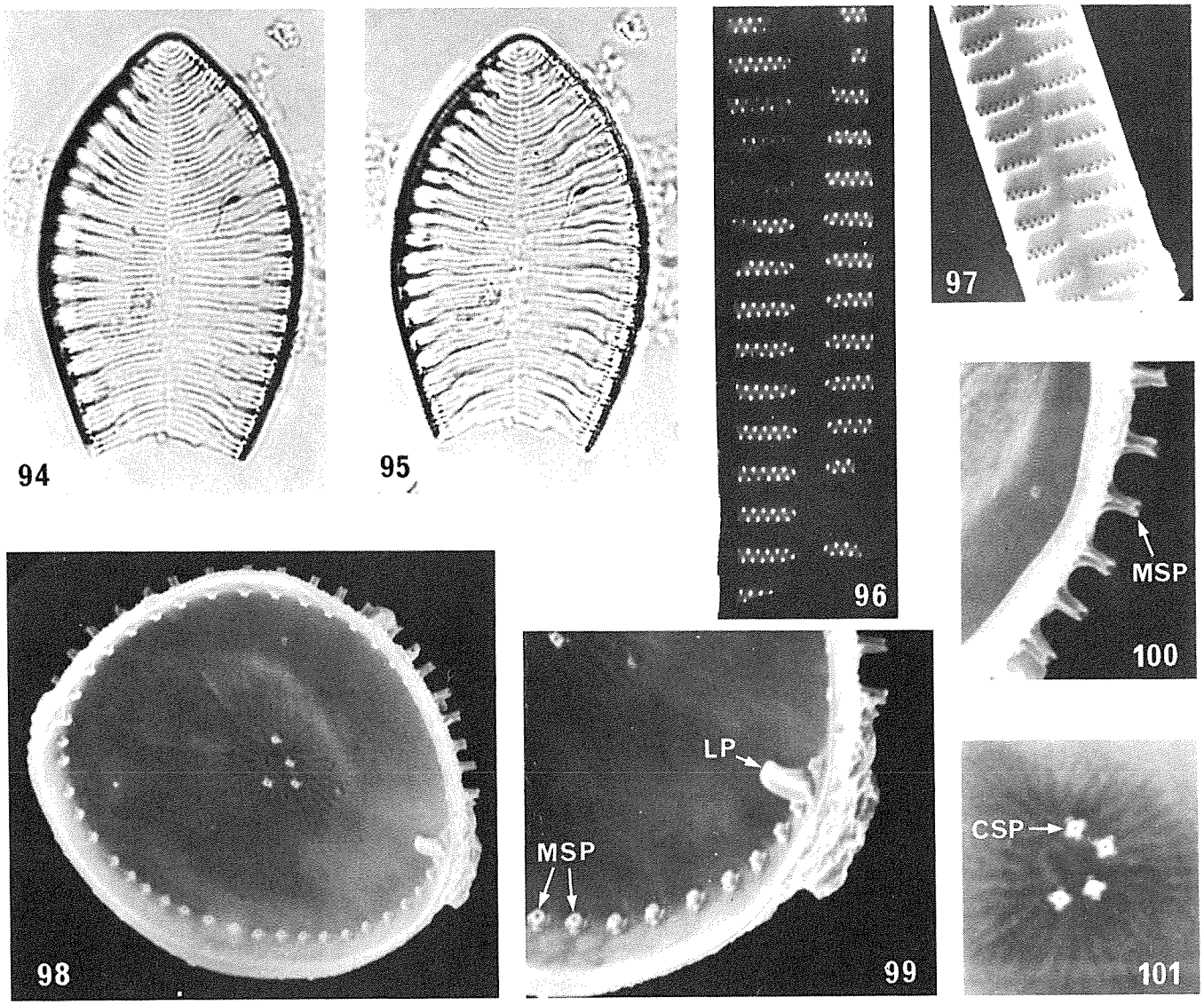

Figures 94–101. **Figures 94, 95** *Surirella ovalis* Brébisson, same specimen, LM (×1 500). **94.** Bright field illumination; **95.** Oblique illumination. **Figure 96** *Synedra ulna* (Nitzsch) Ehrenberg complex, TEM (×6 400). Note that each stria is composed of a double row of pores. **Figure 97** *Synedra ulna* (Nitzsch) Ehrenberg complex, SEM, internal view (×6 000). Striae may consist of single or double rows of pores or both. **Figures 98–101** *Thalassiosira weissflogii* (Grunow) Fryxell & Hasle, SEM, internal views. **98.** Whole valve (×5 000). **99.** Part of valve in 98 enlarged to show the labiate process (LP) and the internal ends of the marginal strutted processes (MSP) (×9 000). **100.** Another part of the valve in 98 enlarged to show the external ends of the marginal strutted processes (MSP) (×9 000). **101.** Enlargement of the central strutted processes (CSP) of another valve (×9 000).

intermediate stages.

A search through the literature revealed that in the majority of cases (EM studies) the striae in the *S. ulna* complex are composed of a single row of pores (Helmcke & Krieger 1953, plate 43; Okuno 1974, plate 840, 841; Gerloff & Helmcke 1977, plate 935; Round 1979, plate 2, figures 7–9, 13; Loseva 1982, plate 32, figures 3, 4 and plate 34, figure 3). Montgomery (1978, plate 191, figure D) on the other hand illustrated a valve of *S. ulna* in which the striae have a double row of alternating pores. A micrograph by Lange-Bertalot (1980b, plate 15, figure 260 as *Fragilaria ulna*) is therefore interesting since it appears to be an intermediate form having striae in which there are double rows of pores near the valve margin but single rows near the axial area. Consequently, the *S. ulna* complex appears to present a wider variation in striae structure, making a further study of this group necessary.
Specimens belonging to the *S. ulna* complex occurred in samples B2, B4 and B7.

Thalassiosira weissflogii (Grunow) Fryxell & Hasle (Figures 98–101)

Fryxell & Hasle 1977, 68, figures 1–15.
Fryxell, Hubbard & Villareal 1981, 48, figures 20–28.
Germain 1981, 42, plate 10, figures 13–16.
Archibald 1983, 325, figures 481–483.
Schoeman & Archibald 1977, no. 2 (as *T. fluviatilis* Hustedt).
Diameter 12,0–18,0 μm. Marginal strutted processes 11–14 in 10 μm; 3–5 central strutted processes. One conspicuous labiate process.

The taxonomy and valve morphology of this species have been discussed in the above-mentioned works. We have included some SEM micrographs of internal valve views (Figures 98–101) to show the labiate process (LP), as well as the marginal (MSP) and central strutted processes (CSP). Both the internal and external ends of the marginal strutted processes are visible in Figure 98, whereas an enlargement of the external ends is presented in Figure 100.
T. weissflogii was observed in sample B2.

In addition to the species discussed in detail above and in the previous two papers (Schoeman & Ashton 1982b; 1983), the following taxa were also recorded from the vicinity of the Pretoria Salt Pan. These are listed below together with the references used in their identification. Sampling localities from which these species were recorded are given in Table 1.

Fragilaria construens (Ehrenberg) Grunow var. *venter* (Ehrenberg) Grunow.
Ref. Patrick & Reimer 1966, 126, plate 4, figures 8, 9.
Melosira granulata (Ehrenberg) Ralfs var. *angustissima* O. Müller.
Ref. Hustedt 1927–30, 250, figure 104d.
Navicula cloacina Lange-Bertalot & Bonik.
Ref. Schoeman & Archibald 1977.
Navicula menisculus Schumann.
Ref. Hustedt 1930, 301, figure 517.
Navicula pupula Kützing (Figure 19).
Ref. Schoeman & Archibald 1979.
Navicula pygmaea Kützing (Figures 56–58).
Ref. Schoeman & Archibald 1980.
Navicula rostellata Kützing.
Ref. Hustedt 1930, 297, figure 502; Patrick & Reimer 1966, 507, plate 48, figure 12 as *N. viridula* var. *rostellata* (Kützing) Cleve.
Navicula tenelloides Hustedt.
Ref. Schoeman & Archibald 1976.
Nitzschia communis Rabenhorst (Figure 24).
Ref. Schoeman & Archibald 1977.
Nitzschia dissipata (Kützing) Grunow.
Ref. Schoeman & Archibald 1976.
Nitzschia fontifuga Cholnoky.
Ref. Archibald 1983, 253, figures 385–391.
Nitzschia perminuta Grunow.
Ref. Lange-Bertalot & Simonsen 1978, plate 9, figure 160.
Nitzschia supralitorea Lange-Bertalot.
Ref. Lange-Bertalot 1979, 215, figures 25–27, 76–78; 1980a, 55, figures 143–145.
Rhopalodia gibberula (Ehrenberg) O. Müller.
Ref. Schoeman & Ashton 1982a, 92, figures 71–74, 138–153.
Stauroneis anceps Ehrenberg.
Ref. Patrick & Reimer 1966, 361, plate 30, figure 1.
Surirella ovalis Brébisson (Figures 94, 95).
Ref. Germain 1981, 388, plate 151, figures 1–12.

Acknowledgements

This paper is published with the approval of the Chief Director of the National Institute for Water Research. Our sincere thanks to Mr H.J. van Tonder for assistance with our SEM studies and Mrs V.H. Meaton who produced the final photographic prints.

References

ANDO, K. 1979. Moss diatoms in Japan (3). *Jap. J. Phycol.* 27: 153–159.
ANONYMOUS. 1975. Proposals for a standardization of diatom terminology and diagnoses. *Nova Hedwigia* Suppl. 53: 323–354.
ARCHIBALD, R.E.M. 1983. The diatoms of the Sundays and Great Fish Rivers in the eastern Cape Province of South Africa. *Biblthca diatomol.* 1: 1–362, 34 pls.
ASHTON, P.J. & SCHOEMAN, F.R. 1983. Limnological studies on the Pretoria Salt Pan, a hypersaline maar lake. I: Morphometric, physical and chemical features. *Hydrobiologia* 99: 61–73.
CHOLNOKY, B.J. 1954. Ein Beitrag zur Kenntnis der Algenflora des Mogolflusses in Nordost-Transvaal. *Öst. bot. Z.* 101: 118–139.
CHOLNOKY, B.J. 1956. Neue und seltene Diatomeen aus Afrika. II. Diatomeen aus dem Tugela — Gebiete in Natal. *Öst. bot. Z.* 103: 53–97.
CHOLNOKY, B.J. 1963. Beiträge zur Kenntnis der Ökologie der Diatomeen des Swakop — Flusses in Südwest-Afrika. *Revta Biol.* 3: 233–260.
COLLINS, G.B. & GROETSCH, C.W. 1981. An elementary mathematical problem arising in Diatom taxonomy. *Int. J. Math. Educ. Sci. Technol.* 12: 121–124.
COMPÈRE, P. 1980. Algues de l'Aïr (Niger). *Bull. Jard. bot. nat. Belg.* 50: 269–329.
COMPÈRE, P. 1981a. Algues des déserts d'Iran. *Bull. Jard. bot. nat. Belg.* 51: 3–40.
COMPÈRE, P. 1981b. Ultrastructural aspects of the frustule of some forms of *Cymbella hustedtii* Krasske. In: Proceedings of the sixth symposium on recent and fossil diatoms, ed. Ross, R. Otto Koeltz, Koenigstein. pp. 155–165.
COX, E.J. 1977. Raphe structure in Naviculoid diatoms as revealed by the scanning electron microscope. *Nova Hedwigia* Suppl. 54: 261–274.
DAWSON, P.A. 1972. Observations on the structure of some forms of *Gomphonema parvulum* Kütz. I. Morphology based on light microscopy, and transmission and scanning electron microscopy. *Br. phycol. J.* 7: 255–271.

DAWSON, P.A. 1973. Observations on some species of the diatom genus *Gomphonema* C.A. Agardh. *Br. phycol. J.* 8: 413–423.
FOGED, N. 1971. Freshwater diatoms in Thailand. *Nova Hedwigia* 22: 267–369.
FOGED, N. 1980. Diatoms in Egypt. *Nova Hedwigia* 33: 629–707.
FRYXELL, G.A. & HASLE, G.R. 1977. The genus *Thalassiosira*: some species with a modified ring of central strutted processes. *Nova Hedwigia* Suppl. 54: 67–98.
FRYXELL, G.A., HUBBARD, G.F. & VILLAREAL, T.A. 1981. The genus *Thalassiosira*: variations of the cingulum. *Bacillaria* 4: 41–63.
GASSE, F. 1980. Les diatomées lacustres pliopléistocènes du Gadeb (Éthiopie). Systématique, paléoécologie, biostratigraphie. *Revue algol.* Suppl. Mém. 3: 1–249.
GERLOFF, J. & HELMCKE, J.-G. 1977. In: Helmcke, J.-G., Krieger, W. & Gerloff, J. 1953–77, Diatomeenschalen im elektronenmikroskopischen Bild, part 10: 1–47, pls 924–1023. J. Cramer, Vaduz.
GERMAIN, H. 1981. Flore des Diatomées (Diatomophycées) eaux douces et saumâtres du Massif Armoricain et des contrées voisines d'Europe occidentale. Société nouvelle des éditions Boubée, Paris. 444 pp.
GERMAIN, H. 1982. Quatre Navicules du groupe des subtilissimae (Diatomophyceae). *Cryptogam. Algol.* 3: 105–111.
HARGRAVES, P.E. & LEVANDOWSKY, M. 1971. Fine structure of some brackish-pond diatoms. *Nova Hedwigia* 21: 321–336.
HELMCKE, J.-G. & KRIEGER, W. 1953. In: Helmcke, J.-G. & Krieger, W. 1953–77, Diatomeenschalen im elektronenmikroskopischen Bild, part 1: 1–20, pls 1–102. Transmare-Photo, Berlin-Wilmersdorf.
HELMCKE, J.-G. & KRIEGER, W. 1954. In: Helmcke, J.-G. & Krieger, W. 1953–77, Diatomeenschalen im elektronenmikroskopischen Bild, part 2: 1–24, pls 103–200. Verlag Bild und Forschung, Berlin-Wilmersdorf.
HUSTEDT, F. 1927–30. Die Kieselalgen. In: Rabenhorst, L. Kryptogamen-Flora von Deutschland, Österreich und der Schweiz, Vol. 7, part 1, 920 pp. Akademische Verlagsgesellschaft m.b.H., Leipzig.
HUSTEDT, F. 1930. Bacillariophyta (Diatomeae). In: Pascher, A. Die Süsswasser-Flora Mitteleuropas, Part 10, 466 pp. G. Fischer, Jena.
HUSTEDT, F. 1931–59. Die Kieselalgen. In: Rabenhorst, L. Kryptogamen-Flora von Deutschland, Österreich und der Schweiz, Vol. 7, Part 2, 845 pp. Akademische Verlagsgesellschaft Geest & Portig K.-G., Leipzig.
HUSTEDT, F. 1937–38. Systematische und ökologische Untersuchungen über die Diatomeen-Flora von Java, Bali und Sumatra. Systematische Teil. *Arch. Hydrobiol.* Suppl. 15: 131–177, 187–295, 393–506.
HUSTEDT, F. 1949a. Diatomeen von der Sinai-Halbinsel und aus dem Libanon-Gebiet. *Hydrobiologia* 2: 24–55.
HUSTEDT, F. 1949b. Süsswasser-Diatomeen. In: Exploration du Parc National Albert, Mission H. Damas (1935–36), Fasc. 8, 199 pp. & 16 pls. M. Hayez, Bruxelles.
HUSTEDT, F. 1961–66. Die Kieselalgen. In: Rabenhorst, L., Kryptogamen-Flora von Deutschland, Österreich und der Schweiz, Vol. 7, Part 3, 816 pp. Akademische Verlagsgesellschaft Geest & Portig K.-G., Leipzig.
KOLBE, R.W. & KRIEGER, W. 1942. Süsswasseralgen aus Mesopotamien und Kurdistan. *Ber. dt. bot. Ges.* 60: 336–355.
KRAMMER, K. 1982a. Valve morphology in the genus *Cymbella* C.A. Agardh. In: Micromorphology of diatom valves, ed. Helmcke, J.-G. & Krammer, K. Vol. XI, 1–49, plates 1024–1148. J. Cramer, Vaduz.
KRAMMER, K. 1982b. Observations on the alveoli and areolae of some Naviculaceae. *Nova Hedwigia* Suppl. 73: 55–79.
KRASSKE, G. 1923. Die Diatomeen des Casseler Beckens und seiner Randgebirge, nebst einigen wichtigen Funden aus Niederhessen. *Bot. Arch.* 3: 185–209.
LANG, J. & PIERRE, J.F. 1974. Contribution a l'etude des diatomees de quelques depots carbonates actuels hydrothermaux et lacustres de l'Afghanistan Central. *Bull. Acad. Soc. Lorraines Sci.* 13: 39–54.
LANGE-BERTALOT, H. 1977. Eine Revision zur Taxonomie der Nitzschiae lanceolatae Grunow. Die 'klassischen' bis 1930 beschriebenen Süsswasserarten Europas. *Nova Hedwigia* 28: 253–307.
LANGE-BERTALOT, H. 1978. Diatomeen-Differentialarten anstelle von Leitformen: ein geeigneteres Kriterium der Gewässerbelastung. *Arch. Hydrobiol.* Suppl. 51: 393–427.
LANGE-BERTALOT, H. 1979. Toleranzgrenzen und Populationsdynamik benthischer Diatomeen bei unterschiedlich starker Abwasserbelastung. *Arch. Hydrobiol.* Suppl. 56: 184–219.
LANGE-BERTALOT, H. 1980a. New species, combinations and synonyms in the genus *Nitzschia*. *Bacillaria* 3: 41–77.
LANGE-BERTALOT, H. 1980b. Zur systematischen Bewertung der bandförmigen Kolonien bei *Navicula* und *Fragilaria*. *Nova Hedwigia* 33: 723–787.
LANGE-BERTALOT, H. & SIMONSEN, R. 1978. A taxonomic revision of the Nitzschiae lanceolatae Grunow. 2. European and related extra-European freshwater and brackish water taxa. *Bacillaria* 1: 11–111.
LEWIN, J.C. & LEWIN, R.A. 1960. Auxotrophy and heterotrophy in marine littoral diatoms. *Can. J. Microbiol.* 6: 127–134.
LOSEVA, E.I. 1982. Atlas of Late-Pliocene diatoms of Prikamje (In Russian), 204 pp. and 104 pls. Leningradskoe Otdelenie, Leningrad.
LOWE, R.L. 1972. Diatom population dynamics in a Central Iowa drainage ditch. *Iowa St. J. Res.* 47: 7–59.
MANN, D.G. 1981. Sieves and flaps: siliceous minutiae in the pores of raphid diatoms. In: Proceedings of the sixth symposium on recent and fossil diatoms, ed. Ross, R. Otto Koeltz, Koenigstein. pp. 279–300.
MAYAMA, S. & KOBAYASI, H. 1982. Diatoms from the Aonogawa River. *Bull. Tokyo Gakugei Univ.* Sect. 4, 34: 77–107.
MEISTER, F. 1932. Kieselalgen aus Asien. Verlag von Gebrüder Borntraeger, Berlin, 56 pp. & 19 pls.
MILLER, U. 1971. Diatom floras in the sediments at Leveäniemi. In: Lundqvist, J. The interglacial deposit at the Leveäniemi Mine, Svappavaara, Swedish Lapland, *Sver. geol. Unders. Afh.* Ser. C658, Arsb. 65: 104–163.
MIZUNO, M. 1982. Change in striation density and systematics of *Cocconeis scutellum* var. *ornata* (Bacillariophyceae). *Bot. Mag., Tokyo* 95: 349–357.
MONTGOMERY, R.T. 1978. Environmental and ecological studies of the diatom communities associated with the coral reefs of the Florida Keys, Vol. 2. Ph.D. thesis, Florida State University, Florida, U.S.A.
OKUNO, H. 1974. Freshwater diatoms. In: Helmcke, J.-G., Krieger, W. & Gerloff, J. 1953–77, Diatomeenschalen im elektronenmikroskopischen Bild, part 9: 1–45, pls 825–923. J. Cramer, Vaduz.
PATRICK, R. & REIMER, C.W. 1966. The diatoms of the United States exclusive of Alaska and Hawaii. Vol. 2. *Monogr. Acad. Nat. Sci. Philad.* 13: 1–688.
PATRICK, R. & REIMER, C.W. 1975. The diatoms of the United States exclusive of Alaska and Hawaii, Vol. 2, Part 1. *Monogr. Acad. Nat. Sci. Philad.* 13: 1–213.
ROSS, R., COX, E.J., KARAYEVA, N.I., MANN, D.G., PADDOCK, T.B.B., SIMONSEN, R. & SIMS, P.A. 1979. An amended terminology for the siliceous components of the diatom cell. *Nova Hedwigia* Suppl. 64: 513–533.
ROUND, F.E. 1979. The classification of the genus *Synedra*. *Nova Hedwigia* Suppl. 64: 135–146.
ROUND, F.E. 1981. The diatom genus *Stephanodiscus*: an electronmicroscopic view of the classical species. *Arch. Protistenk.* 124: 455–470.
ROUND, F.E. 1982. *Cyclostephanos* — a new genus within the Sceletonemaceae. *Arch. Protistenk.* 125: 323–329.
ROUND, F.E. & MANN, D.G. 1981. The diatom genus *Brachysira* I. Typification and separation from *Anomoeoneis*.

Arch. Protistenk. 124: 221–231.

SCHOEMAN, F.R. 1973. A systematical and ecological study of the diatom flora of Lesotho with special reference to the water quality, 355 pp. and 10 pls. V & R Printers, Pretoria.

SCHOEMAN, F.R. & ARCHIBALD, R.E.M. 1976. The diatom flora of southern Africa. No. 1, September 1976. CSIR Special Report WAT 50. No pagination; series of plates with text, 43 pp. Graphic Arts Division of the CSIR, Pretoria.

SCHOEMAN, F.R. & ARCHIBALD, R.E.M. 1977. The diatom flora of southern Africa. No. 2, February 1977. CSIR Special Report WAT 50. No pagination; series of plates with text, 49 pp. Graphic Arts Division of the CSIR, Pretoria.

SCHOEMAN, F.R. & ARCHIBALD, R.E.M. 1979. The diatom flora of southern Africa. No. 5, September 1979. CSIR Special Report WAT 50. No pagination; series of plates with text, 65 pp. Graphic Arts Division of the CSIR, Pretoria.

SCHOEMAN, F.R. & ARCHIBALD, R.E.M. 1980. The diatom flora of southern Africa. No. 6, May 1980. CSIR Special Report WAT 50. No pagination; series of plates with text, 111 pp. Graphic Arts Division of the CSIR, Pretoria.

SCHOEMAN, F.R. & ASHTON, P.J. 1982a. The diatom flora of the Pretoria Salt Pan, Transvaal, Republic of South Africa. *Bacillaria* 5: 63–99.

SCHOEMAN, F.R. & ASHTON, P.J. 1982b. The diatom flora in the vicinity of the Pretoria Salt Pan, Transvaal, Republic of South Africa I. *Nova Hedwigia* Suppl. 73: 21–54.

SCHOEMAN, F.R. & ASHTON, P.J. 1983. The diatom flora in the vicinity of the Pretoria Salt Pan, Transvaal, Republic of South Africa. Part II. *S. Afr. J. Bot.* 2: 191–201.

STOERMER, E.F. & HÅKANSSON, H. 1983. An investigation of the morphological structure and taxonomic relationships of *Stephanodiscus damasii* Hustedt. *Bacillaria* 6: 245–255.

THERIOT, E. & STOERMER, E.F. 1981. Some aspects of morphological variation in *Stephanodiscus niagarae* (Bacillariophyceae). *J. Phycol.* 17: 64–72.